Small molecule proteomics quantifies differences between normal and fibrotic pulmonary extracellular matrices

Xin-Long Wan[1,2], Zhi-Liang Zhou[3], Peng Wang[3], Xiao-Ming Zhou[3], Meng-Ying Xie[4], Jin Mei[5], Jie Weng[3], Hai-Tao Xi[5], Chan Chen[4], Zhi-Yi Wang[2,3,5], Zhi-Bin Wang[5]

[1]Platform for Radiation Protection and Emergency Preparedness of Southern Zhejiang, School of Public Health and Management, Wenzhou Medical University, Wenzhou, Zhejiang 325035, China;

[2]Center for Health Assessment, Wenzhou Medical University, Wenzhou, Zhejiang 325035, China;

[3]Department of Emergency Medicine and General Practice, The Second Affiliated Hospital and Yuying Children's Hospital of Wenzhou Medical University, Wenzhou, Zhejiang 325027, China;

[4]Department of Geriatric Medicine, The First Affiliated Hospital of Wenzhou Medical University, Wenzhou, Zhejiang 325000, China;

[5]Institute of Bioscaffold Transplantation and Immunology, School of Basic Medical Sciences, Wenzhou Medical University, Wenzhou, Zhejiang 325035, China.

Abstract

Background: Pulmonary fibrosis is a respiratory disease caused by the proliferation of fibroblasts and accumulation of the extracellular matrix (ECM). It is known that the lung ECM is mainly composed of a three-dimensional fiber mesh filled with various high-molecular-weight proteins. However, the small-molecular-weight proteins in the lung ECM and their differences between normal and fibrotic lung ECM are largely unknown.

Methods: Healthy adult male Sprague-Dawley rats (*Rattus norvegicus*) weighing about 150 to 200 g were randomly divided into three groups using random number table: A, B, and C and each group contained five rats. The rats in Group A were administered a single intragastric (i.g.) dose of 500 μL of saline as control, and those in Groups B and C were administered a single i.g. dose of paraquat (PQ) dissolved in 500 μL of saline (20 mg/kg). After 2 weeks, the lungs of rats in Group B were harvested for histological observation, preparation of de-cellularized lung scaffolds, and proteomic analysis for small-molecular-weight proteins, and similar procedures were performed on Group C and A after 4 weeks. The differentially expressed small-molecular-weight proteins (DESMPs) between different groups and the subcellular locations were analyzed.

Results: Of the 1626 small-molecular-weight proteins identified, 1047 were quantifiable. There were 97 up-regulated and 45 down-regulated proteins in B *vs.* A, 274 up-regulated and 31 down-regulated proteins in C *vs.* A, and 237 up-regulated and 28 down-regulated proteins identified in C *vs.* B. Both the up-regulated and down-regulated proteins in the three comparisons were mainly distributed in single-organism processes and cellular processes within biological process, cell and organelle within cellular component, and binding within molecular function. Further, more up-regulated than down-regulated proteins were identified in most sub-cellular locations. The interactions of DESMPs identified in extracellular location in all comparisons showed that serum albumin (Alb) harbored the highest degree of node (25), followed by prolyl 4-hydroxylase beta polypeptide (12), integrin β1 (10), apolipoprotein A1 (9), and fibrinogen gamma chain (9).

Conclusions: Numerous PQ-induced DESMPs were identified in de-cellularized lungs of rats by high throughput proteomics analysis. The DESMPs between the control and treatment groups showed diversity in molecular functions, biological processes, and pathways. In addition, the interactions of extracellular DESMPs suggested that the extracellular proteins Alb, Itgb1, Apoa1, P4hb, and Fgg in ECM could be potentially used as biomarker candidates for pulmonary fibrosis. These results provided useful information and new insights regarding pulmonary fibrosis.

Keywords: Small molecular protein; Extracellular matrix; Pulmonary fibrosis; Paraquat; Biomarkers; Rats

Introduction

Pulmonary fibrosis is a progressive lung disease that is refractory to treatment and has a high mortality.[1] It can lead to the development of a permanent fibrotic scar, characterized by excessive accumulation of extracellular matrix (ECM) components.[2-4] If lung fibrosis progresses in an uncontrolled manner, it will result in the irreversible

Access this article online

Quick Response Code:

Website: www.cmj.org

DOI: 10.1097/CM9.0000000000000754

Correspondence to: Dr. Zhi-Bin Wang, Institute of Bioscaffold Transplantation and Immunology, School of Basic Medical Sciences, Wenzhou Medical University, Wenzhou, Zhejiang 325035, China
E-Mail: wangzb@wmu.edu.cn

Chinese Medical Journal 2020;133(10)

Received: 04-11-2019 **Edited by:** Pei-Fang Wei

stiffening of the affected tissue, leading to organ malfunction, gas exchange disruption, and death from respiratory failure.[5] Unfortunately, there are currently no effective therapies to reverse the effects of fibrosis.[6]

Paraquat (1,1'-dimethyl-4,4'-bipyridinium dichloride, PQ) is an extremely effective and non-selective contact herbicide used worldwide in the agricultural and horticultural industries.[7,8] It is a water-soluble organic heterocyclic compound that is highly toxic to humans and animals.[9] PQ absorbed through the skin, the respiratory tract, and the digestive tract can result in multiple organ failure, with the lung being the primary target organ.[10] Lung damage is caused by increasing PQ concentrations in the lung, resulting in free radical generation that triggers inflammatory responses, which initiate an irreversible fibrotic process.[11,12] There is no specific therapy for PQ poisoning other than reducing its absorption, increasing its elimination, and attempting to prevent organ injury.[13] Thus, the mortality rate caused by PQ poisoning is very high.[12,14-16] However, due to its easy access and low price, it is difficult to prevent PQ poisoning. Accidental or voluntary PQ poisoning has become a common cause of death in developing countries where its use is less strictly controlled than in Europe or the United States.[17-19] To define the theoretical basis for developing an effective treatment approach, further studies on the mechanisms of PQ-induced pulmonary injury are warranted.

To date, a few lung proteomic studies in rats have been reported. For example, compared to control rats, 32 differentially expressed proteins (DEPs) were identified in lung tissues of rats exposed to radon and cigarette smoke by matrix-assisted laser desorption/ionization tandem time-of-flight mass spectrometry.[20] Using the same method, 18 DEPs were identified between *Pseudomonas aeruginosa*-infected and native lung tissues.[21] Compared to native lungs, 26, 30, and 37 DEPs were detected in hypobaric-induced hypoxia in rat lungs for 6, 12, and 24 h, respectively, by 2-dimensional gel electrophoresis (2-DE).[22] The de-cellularized scaffold produced by the "triton/sodium dodecyl sulfate (SDS)" de-cellularization method was found to retain similar levels of laminins, proteoglycans, and other ECM-associated proteins to the original lung by using proteotypic ^{13}C-labeled peptides.[23] As a structural support for cells, ECM is highly variable depending on its surroundings. It has been shown that fibrotic lung ECM promoted transformation of fibroblasts into myofibroblasts.[24] However, no proteomic study has been conducted on fibrotic ECM. Particularly, the small-molecular-weight proteins have rarely been studied compared to macromolecule proteins such as collagen, elastin, and proteoglycans. Thus, in this study, we used the isobaric tags for relative and absolute quantification (iTRAQ) technique to identify the small-molecular-weight proteins of fibrotic lung ECM at 2 and 4 weeks following treatment with PQ in comparison with the control. The aims of this study were to identify differences of small-molecular-weight proteins between normal and fibrotic lung ECM and to discover potential biomarker candidates for pulmonary fibrosis. The findings are expected to provide useful information regarding PQ-induced pulmonary fibrosis and new insight for future studies on therapies of lung fibrosis.

Methods

Ethical approval

Animal experiments were performed in the Institute of Bioscaffold Transplantation and Immunology, Wenzhou Medical University, Zhejiang Province, China and approved by the Committee on Ethics regarding Animal Experiments of Wenzhou Medical University (No. SCXK [ZHE] 2010-0044). All rats used in the experiments were treated according to Regulations for the Administration of Affairs Concerning Experimental Animals which were approved by the State Council of China. Every effort was made to reduce the number of animals and minimize their suffering.

Experimental drugs and rats

PQ was purchased from Nanjing Red Sun Co. Ltd (Nanjing, Jiangsu, China) and was used to induce pulmonary fibrosis as described previously.[25] Healthy adult male Sprague-Dawley (SD) rats (*Rattus norvegicus*) purchased from the SLAC Laboratory Animal Co., Ltd (Shanghai, China) weighing about 150 to 200 g were randomly divided into groups A, B, and C using random number table, and each group contained five rats. The rats in Group A were administered a single intragastric (i.g.) dose of 500 μL of saline as control, and those in Groups B and C were administered a single i.g. dose of PQ dissolved in 500 μL of saline (20 mg/kg). After 2 weeks of treatment, the lungs of rats in Group B were harvested for histological observation and preparation of de-cellularized lung scaffolds, while these experiments were performed for the rats of Groups C and A after 4 weeks.

Histological examination for fibrosis and de-cellularization of lung matrices

The abdominal cavities of all anesthetized rats were opened and the inferior vena cava was separated to be exposed to the operator, and then heparin saline (Sigma, Munich, Germany) was intravenously injected to all rats through the vena cava. The chest was opened and tissues around the lung and heart were removed. The trachea, thoracic aorta, and vena cava were transected to obtain the lung and heart. All lungs and hearts were immersed in phosphate buffer saline (PBS) consisting of 1% penicillin and streptomycin (Gibco) at 4°C. To identify pulmonary fibrosis induced by PQ, native and poisoned lungs were fixed with 4% paraformaldehyde. Hematoxylin and eosin (H&E) (Sigma) and Masson's trichrome (Sigma) staining were conducted on 5 μm sections to detect fibrosis. Images were acquired with an optical microscope (ECLIPSE Ci-L Nikon, Tokyo, Japan). The de-cellularization of lung matrices was performed by perfusion through the pulmonary artery with 500 mL of 1% Triton X-100 (Sigma), followed by 500 mL of sterile distilled water and 2000 mL of 0.8% SDS (Sigma) with a flow rate of 6 mL/min. Next, sterile distilled water was perfused to the lungs for at least

12 h with a flow rate of 2 mL/min. Finally, the scaffolds were washed with PBS containing antibiotics (100 U/mL penicillin G, 100 U/mL streptomycin, and amphotericin B; Boyun Biotech Co., Ltd, Shanghai, China) for 12 h as described in a previous study.[26]

Protein extraction

The frozen tissues were powered with liquid nitrogen and lysed in 8 mol/L urea, 50 mmol/L Tris (pH 8.0), 1% Nonidet P-40 (NP-40), 1% sodium deoxycholate supplemented with 5 mmol/L dithiothreitol, 2 mmol/L ethylene diamine tetra-acetic acid and protease inhibitor cocktail (Calbiochem, Darmstadt, Germany). After sonication on ice, unbroken cells and debris were removed by centrifugation at 4°C for 10 min at 20,000×*g*. Protein content in the supernatant was determined with 2D Quant kit (GE Healthcare Life Science, Beijing, China) according to the instructions.

iTRAQ labeling, fractionation by basic reverse-phase chromatography and liquid chromatography-electrospray ionization-mass spectrometry (LC-ESI-MS/MS) analysis by Q Exactive Plus

Peptides were reconstituted in 20 μL of 0.5 mol/L tetraethyl ammonium bromide and processed according to the manufacturer's protocol for iTRAQ 8 plex kit (AB Sciex, Boston, MA, USA). The labeled peptides were pooled and reconstituted in buffer A (2% acrylonitrile [ACN], 0.1% fatty acids [FA]) and loaded onto a 4.6 × 250 mm X Bridge Shield C18 reversed phase (RP) column containing 3.5 μm particles (Waters, Milford, USA) with LC20AD high performance liquid chromatography (Shimadzu, Kyoto, Japan). The peptides were eluted at a flow rate of 1 mL/min with a gradient of buffer B (80% ACN, pH 10.0): 5% to 12% for 20 min, 12% to 35% for 45 min, and 35% to 80% for 5 min. The system was then maintained in buffer B for 5 min before equilibrating with 5% buffer B. Elution was monitored by measuring absorbance at 214 nm, and fractions were collected every minute. The eluted peptides were pooled as 20 fractions and vacuum-dried.

The lyophilized peptides were resuspended in buffer A (2% ACN, 0.1% FA), loaded onto an Acclaim PepMap 100 C18 trap column (75 μm × 2 cm; Dionex, Sunnyvale, CA, USA) by ultimate 3000 nano ultra-high performance liquid chromatography (UPLC) (Dionex) and eluted onto an Acclaim PepMap rapid separation liquid chromatography (RSLC) C18 analytical column (75 μm × 25 cm; Dionex). A 45 min linear gradient was run at 300 nL/min, starting from 11% to 20% buffer B (80% ACN, 0.1% FA), followed by 2 min gradient to 80% buffer B, and maintenaned at 80% buffer B for 3 min.

The peptides were subjected to nanospray ion source in mass spectrometry Q Exactive plus (Thermo Scientific, Waltham, MA, USA) coupled online to the UPLC according to the manufacturer's protocol.

Small-molecular-weight protein identification and quantification

Considering that the high-molecular-weight proteins in ECM have been well studied, only small-molecular-weight proteins were identified and quantified. In this study, proteins with molecular weight ranging from 6.0 to 1025 kDa were examined. The resulting raw data were converted to mascot generic file with Proteome Discoverer v1.4.1.14 (Thermo Scientific) and processed using Mascot Search Engine ver 2.3.02 (Matrix Science, Boston, MA, USA). Tandem mass spectra were searched against swissprot mouse database (16,724 sequences). Mass error was set to 10 parts per million (ppm) for precursor ions and 0.02 Da for fragments. Trypsin was selected for enzyme specificity and two missed cleavages were allowed. Carbamido methylation on cysteine, iTRAQ 8-plex tag on lysine, and peptide N-terminal were specified as fixed modification, and oxidation on methionine and iTRAQ 8-plex tag on tyrosine were specified as variable modification. Decoy (reverse) database was searched against to estimate false discovery rate. The calculating results were revalued by algorithm percolator, and peptide-spectrum matches with $P < 0.05$ and $e < 0.05$ were accepted. For quantification, a small-molecular-weight protein must have at least two unique peptides above identity. The pair-wise Pearson correlations between groups were calculated by MATLAB 9.0 (MathWorks, Natick, MA, USA).

Bioinformatics analysis

Gene Ontology (GO) annotation of all identified proteins originated from the UniProt-GOA database (http://www.ebi.ac.uk/GOA/). The proteins were annotated using the InterProScan software by aligning the protein sequences. The sub-cellular localizations of all identified proteins were determined by the software PSORT/PSORT II (http://www.genscript.com/wolf-psort.html). GO of all differentially expressed small-molecular-weight proteins (DESMPs) were analyzed.

Protein-protein interaction (PPI) network

To obtain the interactions of DESMPs in ECM, all identified protein name identifiers were searched against the Search Tool for the Retrieval of Interacting Genes/Proteins (STRING) database version 9.1 (https://string-db.org) for PPIs. Only the interactions between proteins that belong to the searched data set were selected, thereby excluding external candidates. STRING uses a metric called "confidence score" to define the interaction confidence; all interactions that had a confidence score ≥0.7 (high confidence) were selected. Interaction network from STRING was visualized in Cytoscape (https://cytoscape.org).

Results

Identification of pulmonary fibrosis

H&E and Masson trichrome staining were used to evaluate the histological changes induced by PQ at 2 weeks. The H&E staining results showed that PQ induced an inflammatory response characterized by thickened alveolar septa with a considerable number of interstitial cells and broken alveoli compared to controls,

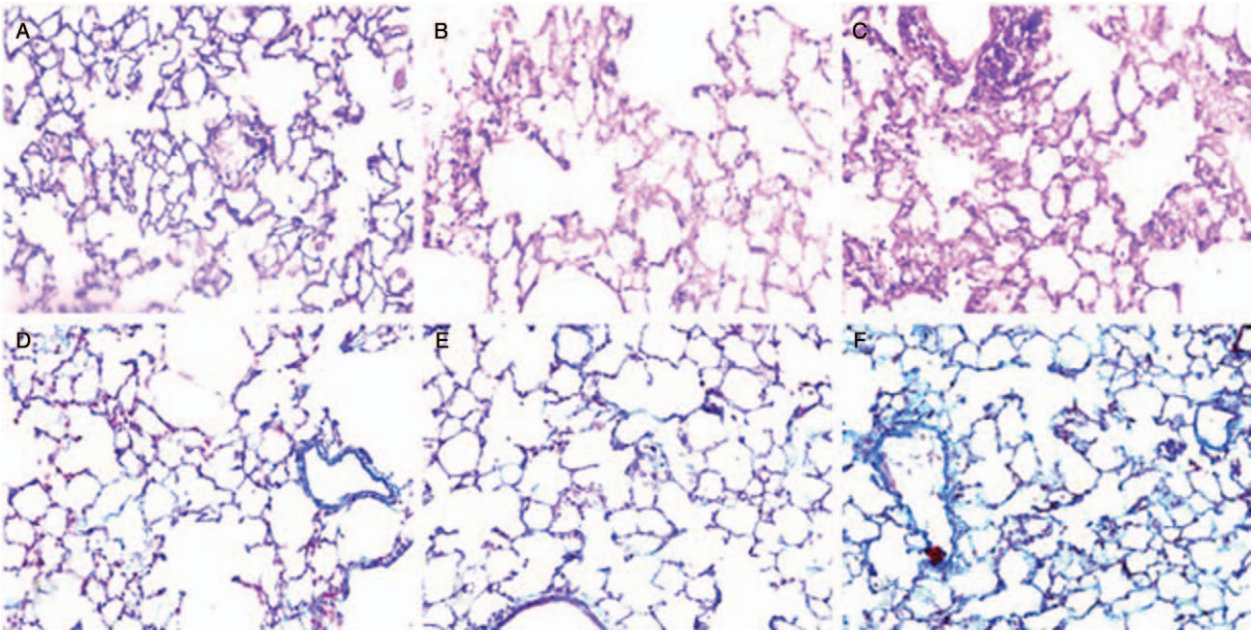

Figure 1: H&E and Masson staining of normal and fibrotic lung tissues (original magnification ×100). (A) H&E staining of normal lung tissue. (B) H&E staining of fibrotic lung tissue (2 weeks). (C) H&E staining of fibrotic lung tissue (4 weeks). (D) Masson staining of normal lung tissue. (E) Masson staining of fibrotic lung tissue (2 weeks). (F) Masson staining of fibrotic lung tissue (4 weeks). H&E: Hematoxylin-eosin.

which became more serious after 4 weeks of induction [Figure 1A–C]. Masson trichrome staining further revealed an increased collagen accumulation, especially in the thickened alveolar regions and small bronchioles in PQ-treated lung after 2 weeks compared to the control group, and collagen accumulation increased further after 4 weeks [Figure 1D–F]. These phenomena were consistent with pulmonary inflammation, which resulted in pulmonary fibrosis.

Quality verification of the mass spectrum (MS) data

To quantify the fluctuation in small-molecular-weight proteins of different de-cellularized lung samples, diverse proteomic approaches were conducted. The pair-wise Pearson's correlation showed few variations between repeated samples, suggesting that this method was highly repeatable [Figure 2A]. In quantification, it is important to enhance the precision and credibility of the results when a protein harbors multi-peptides. In this study, most proteins harbored more than two peptides, suggesting accurate protein quantification [Figure 2B]. Most peptides in this study were composed of 5 to 18 amino acid residues, suggesting a general standard sample preparation [Figure 2C]. Furthermore, the first-order mass error in most MS data was within 0.01 Da, which was confirmed to be the characteristic of high accuracy of orbital well mass spectrum [Figure 2D]. This indicated that the mass accuracy of MS was normal, suggesting that protein quantification would not be likely to be affected by the mass errors. Furthermore, the protein coverage distribution, the protein mass distribution and negative relationships between protein mass and protein coverage also indicated that the MS data were reliable [Supplementary Figure 1, http://links.lww.com/CM9/A203].

Summary of the MS data

A total of 6930 peptides and 1626 small-molecular-weight proteins were identified from the whole proteomic data, which included 6387 unique peptides and 1047 quantifiable small-molecular-weight proteins, respectively.

In the comparison of group B *vs.* A, 142 DESMPs, including 97 up-regulated and 45 down-regulated proteins, were identified. The DESMPs between C and A were composed of 274 up-regulated and 31 down-regulated proteins, and there were 237 up-regulated and 28 down-regulated proteins in the comparison of group C *vs.* B. Consistently, the number of up-regulated proteins was higher than that of down-regulated proteins in all comparisons.

Distribution of DESMPs in GO annotation and sub-cellular location

The distributions of up-regulated and down-regulated proteins in GO annotation in comparisons of B *vs.* A, C *vs.* A, and C *vs.* B are shown in Figure 3. Overall, both the up-regulated and down-regulated proteins in the three comparisons were richly distributed in single-organism processes and cellular processes within biological process, cell and organelle within cellular components, and binding within molecular function [Figure 3]. In detail, in the B *vs.* A comparison, there were 66 up-regulated and 27 down-regulated proteins in single-organism processes, 60 up-regulated and 24 down-regulated proteins in cellular processes concerning biological process terms, 83 up-regulated and 25 down-regulated proteins in cell, 77 up-regulated and 22 down-regulated proteins in organelle concerning cellular component, 66 up-regulated and

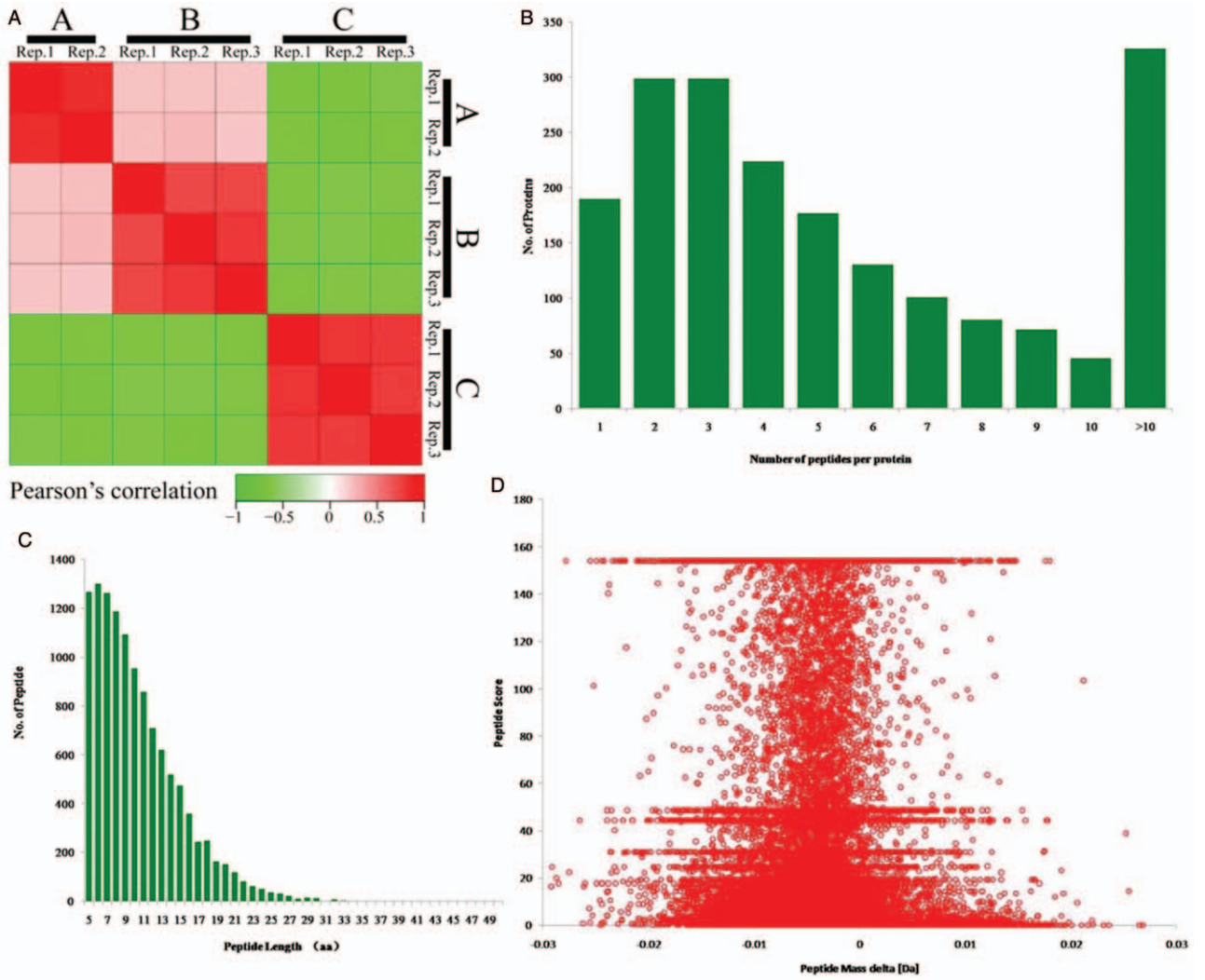

Figure 2: Quality validation of the mass spectrum data. (A) Pearson correlation of protein quantitation. (B) Peptide number distribution of all identified proteins. (C) Length distribution of all identified peptides. (D) Mass delta of all identified peptides.

28 down-regulated proteins in binding concerning molecular function [Figure 3A]. Likewise, both the comparisons of C *vs.* A and C *vs.* B showed a pattern of distribution of up-regulated and down-regulated proteins similar to that found in the B *vs.* A comparison [Figure 3B and 3C].

Regarding the distribution in sub-cellular location, a higher number of up-regulated proteins compared to down-regulated proteins was observed in most sub-cellular locations [Figure 4]. In the B *vs.* A comparison, up-regulated proteins were highly enriched in sub-cellular locations in the cytoplasm (26 proteins), extracellular (24 proteins), and mitochondria (26 proteins) while down-regulated proteins were enriched in cytoplasm (14 proteins) and extracellular (11 proteins) [Figure 4A]. In the C *vs.* A comparison, most up-regulated and down-regulated proteins were distributed in cytoplasm (103 proteins) and extracellular (13 proteins), respectively [Figure 4B]. In the C *vs.* B comparison, the numbers of up-regulated proteins in cytoplasm and down-regulated proteins in extracellular were 94 and 14, respectively, higher than those in other locations [Figure 4C].

The extracellular DESMPs identified in lung ECM

From all DESMPs, we selected those annotated in extracellular locations. The number of extracellular DESMPs in lung ECM in different comparisons was variable. In the B *vs.* A comparison, there were 32 DESMPs including 21 up-regulated and 11 down-regulated proteins. In the C *vs.* A comparison, there were 53 DESMPs consisting of 40 up-regulated and 13 down-regulated proteins. In the C *vs.* B comparison, there were 55 DESMPs composed of 40 up-regulated and 15 down-regulated proteins. These results showed that the number of up-regulated proteins was higher than that of down-regulated proteins in all comparisons. Among them, 15 DESMPs were found in both C *vs.* A and B *vs.* A, 23 DESMPs in both C *vs.* A and C *vs.* B, and 7 DESMPs in both C *vs.* B and B *vs.* A [Figure 5]. Additionally, seven DESMPs were detected in all comparisons of C *vs.* A, C *vs.* B, and B *vs.* A [Figure 5].

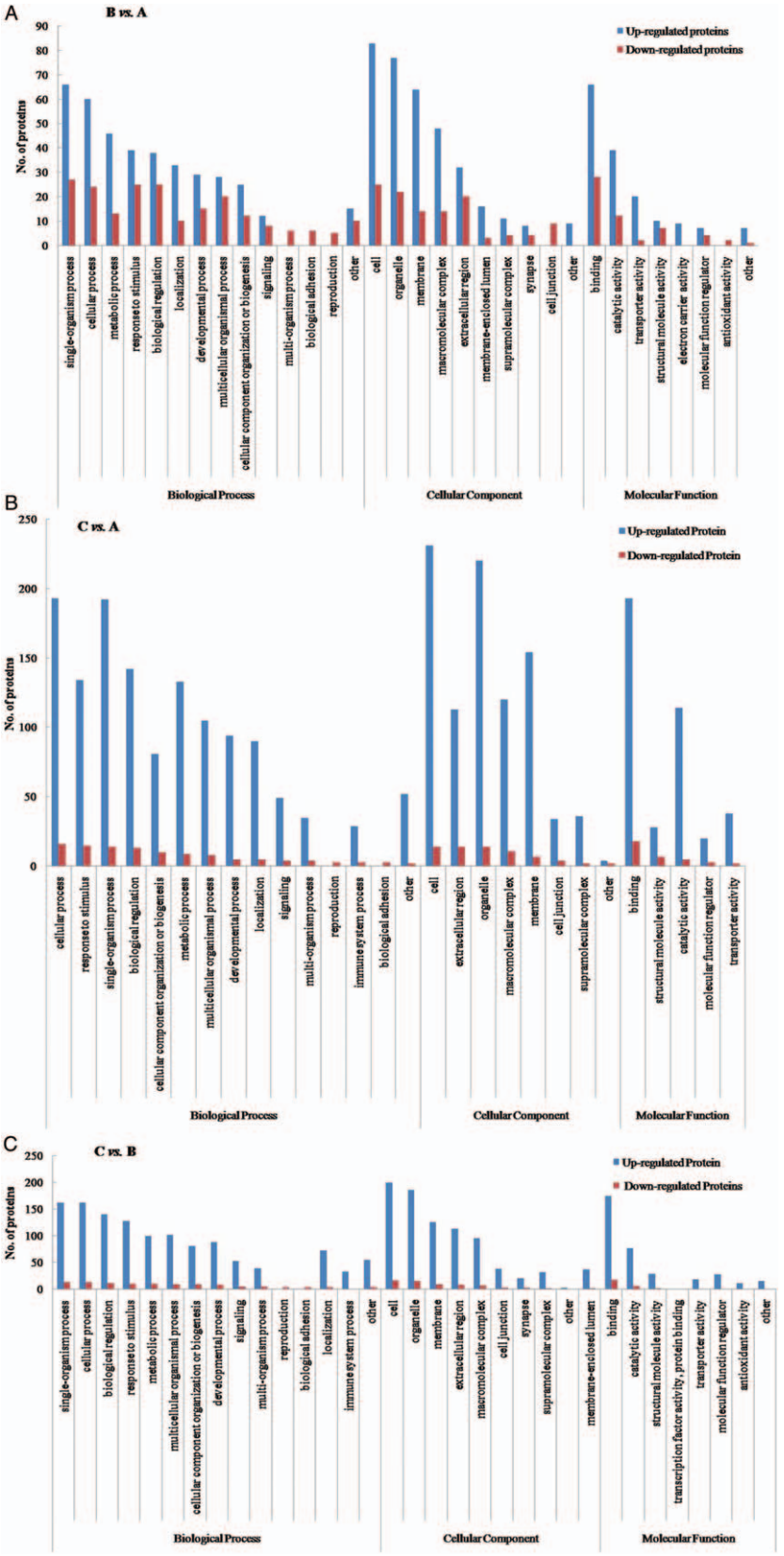

Figure 3: Distribution of down-regulated and up-regulated proteins in GO secondary annotation in the comparison of B *vs.* A (A), C *vs.* A (B), and C *vs.* B (C). A: Control; B: Rats 2 weeks after poisoning with PQ; C: Rats 4 weeks after poisoning with PQ. GO: Gene ontology; PQ: Paraquat.

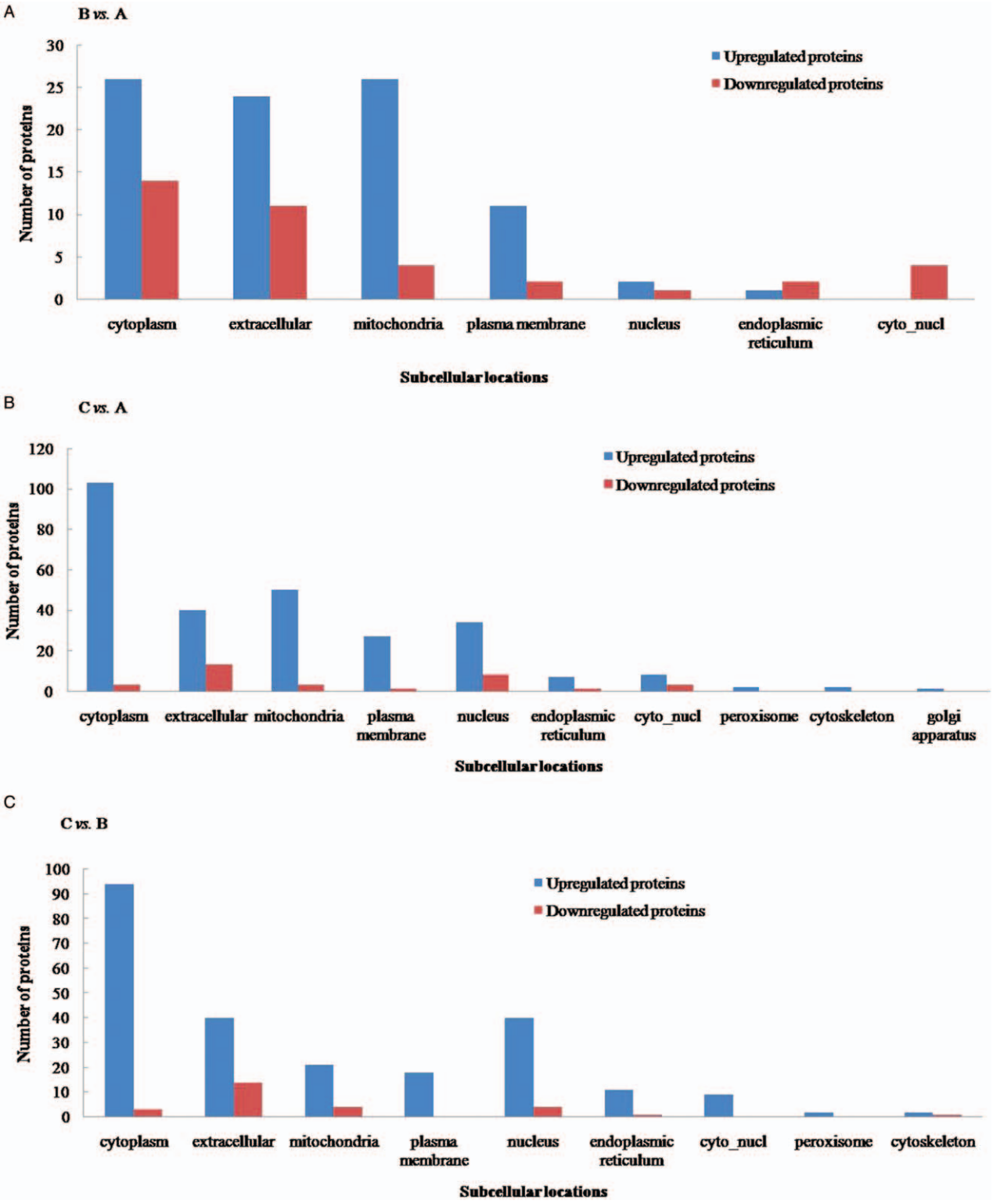

Figure 4: Distribution of down-regulated and up-regulated proteins in sub-cellular locations in the comparison of B *vs.* A (A), C *vs.* A (B), and C *vs.* B (C). A: Control; B: Rats 2 weeks after poisoning with PQ; C: Rats 4 weeks after poisoning with PQ. PQ: Paraquat.

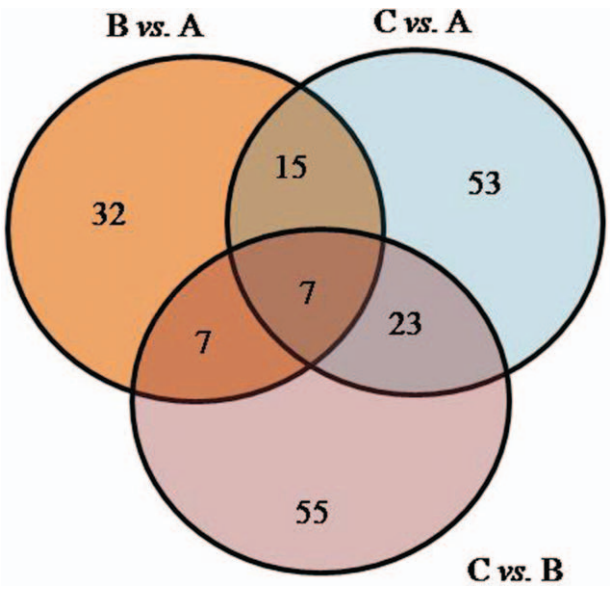

Figure 5: Venn diagram showing the numbers of DESMPs in ECM in different comparisons. A: Control; B: Rats 2 weeks after poisoning with PQ; C: Rats 4 weeks after poisoning with PQ. DESMPs: Differentially expressed small-molecular-weight proteins; ECM: Extracellular matrix; PQ: Paraquat.

The interactions of DESMPs in ECM

The PPIs of the identified DESMPs in ECM were analyzed using Cytoscape software. A network of ECM proteins was created, wherein 57 ECM proteins in the comparisons of B *vs.* A, C *vs.* A, and C *vs.* B were defined as nodes in the PPI network [Figure 6]. This may provide an insight into interactions of DESMPs in the lung ECM of rats. The degree of node refers to the number of edges connected to the node and plays an important role in the evaluation of the relationships of proteins in the network. In this study, the degree of each protein was calculated in the PPI network [Supplementary Table 1, http://links.lww.com/CM9/A204]. Serum albumin (Alb) harbored the highest degree of node (25), followed by prolyl 4-hydroxylase beta polypeptide (P4hb) (10), integrin β1 (Itgb1) (10), apolipoprotein A1 (Apoa1) (9) and fibrinogen gamma chain (Fgg) (9).

Discussion

The lungs, the primary organs of the respiratory system in animals, play an important role in the process of gaseous exchange between the atmosphere and bloodstream. Pulmonary fibrosis makes breathing difficult for human and animals, eventually leading to respiratory and heart failure, or other diseases. It is believed that exposure to some chemicals and smoking and intake of some drugs such as PQ and bleomycin may cause pulmonary fibrosis by acute intoxication or long-term accumulation.[27-33] In this study, histological examinations showed that PQ treatment caused pulmonary fibrosis in rats at two weeks, and it became more serious at four weeks, suggesting that a model of pulmonary fibrosis was successfully established. These results are consistent with previous studies.[34-36] The comparative analysis of small-molecular-weight proteins revealed that PQ induced many DESMPs in lung ECM exhibiting diverse GO terms. The interactions of extracellular DESMPs in ECM inferred that several major proteins (Alb, Apoa1, Itgb1, P4hb, and Fgg) were probably involved in regulating pulmonary fibrosis induced by PQ.

Several studies have performed comparative proteomic analyses in healthy lung tissues and in lungs with drug-induced fibrosis in diverse organisms. For example, Ohlmeier *et al*[37] have analyzed the receptor for advanced glycation end products (RAGE) in human idiopathic pulmonary fibrosis (IPF) and chronic obstructive pulmonary disease (COPD) by 2-DE, mass spectrometry and western blotting and revealed that the full length-RAGE and the C-terminal processed RAGE in both IPF and COPD patients were down-regulated, and endogenous secretory RAGE was down-regulated only in IPF but had no changes in COPD. Another study has identified by 2-DE and matrix assisted laser desorption/ionisation time-of-flight mass spectrometry that 51 DESMPS were up-regulated and 38 were down-regulated in IPF compared to transplant donor lungs, in which up-regulated proteins were heat-shock proteins and DNA damage stress markers while down-regulated proteins in IPF were anti-oxidants, the annexin family, and structural epithelial proteins.[38] A proteomic analysis of ECM in bleomycin-induced pulmonary fibrosis in mice revealed that some unique matrix proteins were synthesized extremely fast during early and late fibrotic response and diverse kinetic pools of pulmonary collagen presented *in vivo* with altered turnover rates during fibrotic evolution.[39] Another proteomic study on familial and sporadic IPF has identified 22 DEPs between familial and sporadic samples, and the up-regulated proteins in familial IPF were involved in several functions such as wounding and immune responses and coagulation system while the up-regulated proteins in sporadic IPF were involved in the oxidative stress response.[40] A proteomic study on lung tissues from bleomycin-treated and native SD rats has identified 88 up-regulated and 58 down-regulated proteins in pulmonary fibrotic tissues, most of which were involved in metabolism, damage response, vitamin A synthesis, and inflammation.[41] The human ECM in the lungs of COPD and IPF has been characterized by quantitative proteomic analysis and the results showed that the proteins regulating endopeptidase activity, as well as those belonging to the serpin family were up-regulated.[42] In our study, 97 up-regulated and 45 down-regulated proteins were identified in PQ-treated rats at early stage (after 2 weeks), and 274 up-regulated and 31 down-regulated proteins at late stage (after 4 weeks), showing more up-regulated proteins than down-regulated proteins. The number of up-regulated proteins increased with prolonged poisoning time, suggesting that PQ induced up-regulation of ECM proteins. The molecular functions of these DESMPs in both comparisons of B *vs.* A and C *vs.* A were mainly classified into binding and catalytic activity, and the subcellular locations were mostly enriched in cytoplasm rather than extracellular.

To analyze the PPI in ECM, we identified and selected 57 extracellular proteins from all DESMPs in the three

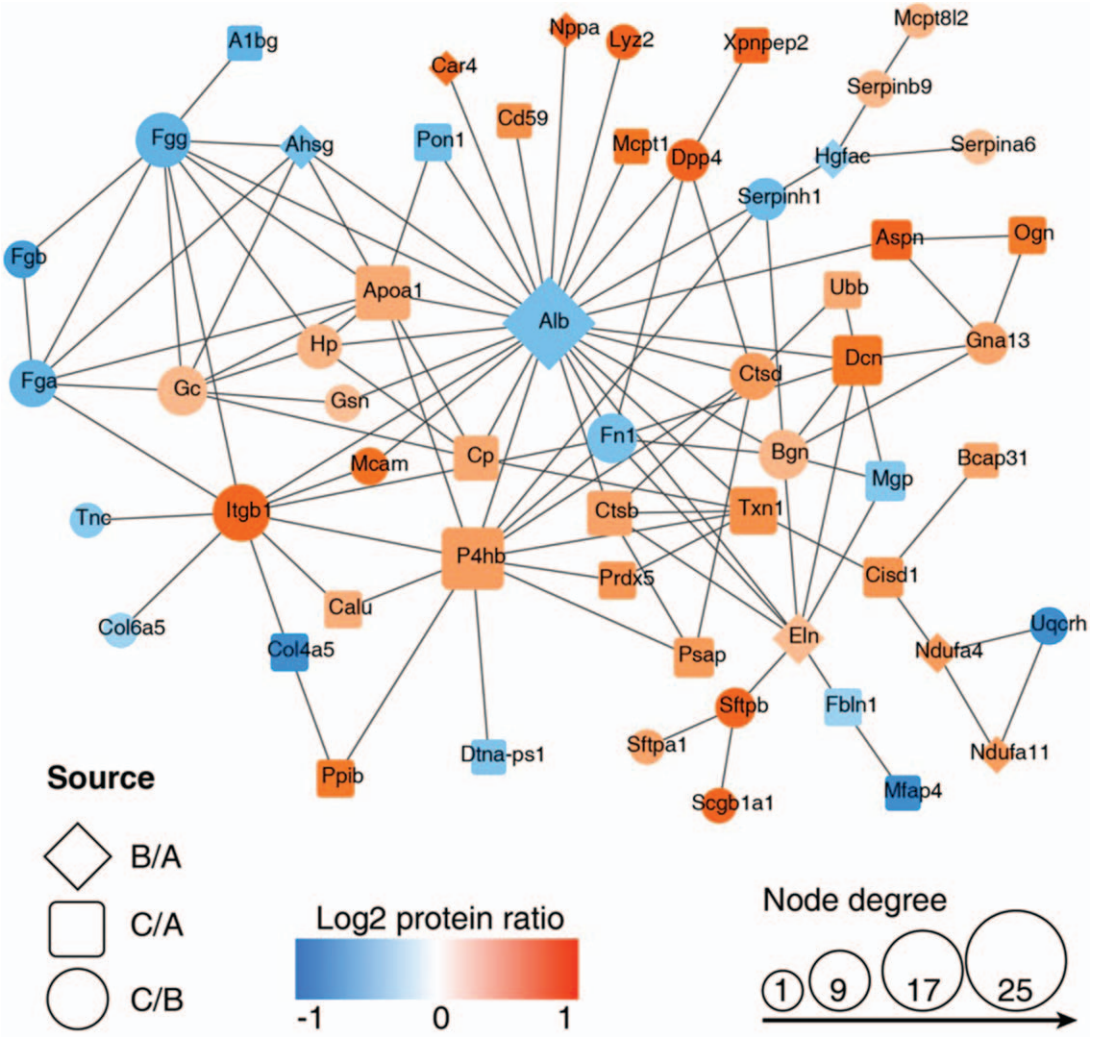

Figure 6: Protein-protein interaction networks for the DESMPs in ECM in the comparisons of B *vs.* A, C *vs.* A, and C *vs.* B were analyzed using Cytoscape software version 3.6.1 (http://cytoscape.org/). A: Control; B: Rats 2 weeks after poisoning with PQ; C: Rats 4 weeks after poisoning with PQ. DESMPs: Differentially expressed small-molecular-weight proteins; ECM: Extracellular matrix; PQ: Paraquat.

comparisons. Similar to the whole data, the up-regulated proteins were also dominant in ECM compared to down-regulated proteins. The interactions of these proteins showed that the top five proteins harboring the highest node degrees were Alb, P4hb, Itgb1, Apoa1, and Fgg, suggesting that they may be potential biomarker candidates for pulmonary fibrosis in rats. Among these biomarkers, Itgb1 has attracted more and more attention due to its wide distribution in ECM and cell surface, as well as its bidirectional channels for mechanical and biochemical signal transmission, responding to intracellular and extracellular stimulation.[43] Integrins are isodimer transmembrane glycoproteins, composed of two sub-units, alpha (120–185 kD) and beta (90–110 kD).[43,44] Integrin β1 as the receptor for fibronectin, laminin, and collagen is widely distributed on the surface of fibroblast and hepatic stellate cells, closely related to tissue and organ fibrosis.[45] It was hypothesized that Itgb1-mediated activation of the mechanochemical conduction pathway focal adhesion kinase-Src-p130^{cas} may initiate multiple downstream signaling pathways and promote transformation of human lung fibroblast lines into muscle fibroblasts, producing amounts of proteins, further aggravating pulmonary interstitial fibrosis.[46] Thus, Itgb1 could be used as an ideal biomarker for identification of pulmonary fibrosis. Additionally, Alb functions primarily as a carrier protein for thyroid hormones, FA, and steroids in the blood and plays a major role in stabilizing extracellular fluid volume by contributing to colloid osmotic pressure of plasma. Alb has been regarded as one of the peripheral blood biomarkers in IPF with low concentrations being associated with increased mortality.[47] P4hb (protein disulfide-isomerase) is an enzyme, located in the endoplasmic reticulum in eukaryotes and in the periplasm of bacteria, which catalyzes the formation, breakage, and rearrangement of disulfide bonds and has been found to regulate allergen-induced fibrosis.[48] The Apoa1 plays important roles in anti-inflammation and anti-fibrotic processes in lung injury and fibrosis induced by bleomycin in mice.[49] The development of pulmonary fibrosis in mice with fibrinogen-deficiency suggested that

Fgg may play a role in the early acute inflammation rather than in collagen deposition at the later stage of the diseases.[50] These studies have shown that the above proteins can be used as biomarkers for IPF, consistent with our inference based on PPI in ECM. Regarding our study, further verification of these biomarkers for pulmonary fibrosis induced by PQ or other drugs is warranted.

The application of proteomic analysis is feasible not only to reveal disease-specific mechanisms but also to discover biomarkers for IPF. For example, a recent proteomic study on IPF using iTRAQ coupled with 2D liquid chromatography-tandem mass spectrometry (LC-MS/MS) method has found that C-reactive protein (CRP), fibrinogen-α chain, haptoglobin, and kininogen-1 could be used as biomarker candidates for IPF.[51] A bronchoalveolar lavage proteomic analysis has suggested that Apoa1, C3a, 14-3-3ε, pulmonary surfactant–associated protein A2 (SPFA2), and S100A6 proteins may be potential biomarkers for pulmonary fibrosis associated with systemic sclerosis.[52] By iTRAQ-based proteomic and proteomic array analysis, Niu *et al*[53,54] have found that alpha-2-HS glycoprotein, alpha-1-microglobulin/bikunin, CRP, and kininogen can be potentially used as IPF biomarkers. Thus, proteomic analysis by various methods may be helpful to discover potential biomarkers for the progression and treatment response of IPF.

In conclusion, numerous PQ-induced DESMPs were identified in de-cellularized lungs of rats by high throughput proteomics analysis. The DESMPs between the control and treatment group showed diversity in molecular functions, biological processes, and pathways. In addition, the interactions of extracellular DESMPs suggested that the extracellular proteins Alb, Itgb1, Apoa1, P4hb, and Fgg in ECM could be potentially used as biomarker candidates for pulmonary fibrosis. These results provided useful information and new insights regarding pulmonary fibrosis.

Funding

This study was supported by grants from the Zhejiang Provincial Natural Science Foundation of China (No. LQ17H010004 and No. LQ16H040002), the National Natural Science Foundation of China (No. 81772054 and No. 81701379), the Zhejiang Medicines Health Science and Technology Program (No. 2016KYB189), and the Wenzhou Science and Technology Bureau Program (No. Y20170179).

Conflicts of interest

None.

References

1. Hutchinson J, Fogarty A, Hubbard R, McKeever T. Global incidence and mortality of idiopathic pulmonary fibrosis: a systematic review. Eur Respir J 2015;46:795–806. doi: 10.1183/09031936.00185114.
2. Murtha LA, Schuliga MJ, Mabotuwana NS, Hardy SA, Waters DW, Burgess JK, *et al*. The processes and mechanisms of cardiac and pulmonary fibrosis. Front Physiol 2017;8:777. doi: 10.3389/fphys.2017.00777.
3. Wynn TA. Integrating mechanisms of pulmonary fibrosis. J Exp Med 2011;208:1339–1350. doi: 10.1084/jem.20110551.
4. Selman M, Pardo A. Revealing the pathogenic and aging-related mechanisms of the enigmatic idiopathic pulmonary fibrosis. An integral model. Am J Respir Crit Care Med 2014;189:1161–1172. doi: 10.1164/rccm.201312-2221PP.
5. Wolters PJ, Collard HR, Jones KD. Pathogenesis of idiopathic pulmonary fibrosis. Annu Rev Pathol 2014;9:157–179. doi: 10.1146/annurev-pathol-012513-104706.
6. Todd NW, Atamas SP, Luzina IG, Galvin JR. Permanent alveolar collapse is the predominant mechanism in idiopathic pulmonary fibrosis. Expert Rev Respir Med 2015;9:411–418. doi: 10.1586/17476348.2015.1067609.
7. Baltazar T, Dinis-Oliveira RJ, Duarte JA, de Lourdes Bastos M, Carvalho F. Paraquat research: do recent advances in limiting its toxicity make its use safer? Br J Pharmacol 2013;168:44–45. doi: 10.1111/j.1476-5381.2012.01870.x.
8. Xiao ZW, Zhang W, Ma L, Qiu ZW. Therapeutic effect of magnesium isoglycyrrhizinate in rats on lung injury induced by paraquat poisoning. Eur Rev Med Pharmacol Sci 2014;18:311–320.
9. Elenga N, Merlin C, Le Guern R, Kom-Tchameni R, Ducrot YM, Pradier M, *et al*. Clinical features and prognosis of paraquat poisoning in French Guiana: a review of 62 cases. Medicine (Baltimore) 2018;97:e9621. doi: 10.1097/MD.0000000000009621.
10. Watts M. Paraquat. Penang, Malaysia: Pesticide Action Network Asia and the Pacific; 2011. 1–43.
11. Dinis-Oliveira RJ, Duarte JA, Sánchez-Navarro A, Remião F, Bastos ML, Carvalho F. Paraquat poisonings: mechanisms of lung toxicity, clinical features, and treatment. Crit Rev Toxicol 2008;38:13–71. doi: 10.1080/10408440701669959.
12. Sun B, Chen YG. Advances in the mechanism of paraquat-induced pulmonary injury. Eur Rev Med Pharmacol Sci 2016;20:1597–1602.
13. Li S, Zhao D, Li Y, Gao J, Feng S. Arterial lactate in predicting mortality after paraquat poisoning: a meta-analysis. Medicine (Baltimore) 2018;97:e11751. doi: 10.1097/MD.0000000000011751.
14. He F, Zhou A, Feng S, Li Y, Liu T. Mesenchymal stem cell therapy for paraquat poisoning: a systematic review and meta-analysis of preclinical studies. PLoS One 2018;13:e0194748. doi: 10.1371/journal.pone.0194748.
15. Li LR, Sydenham E, Chaudhary B, Beecher D, You C. Glucocorticoid with cyclophosphamide for paraquat-induced lung fibrosis. Cochrane Database Syst Rev 2014;8:CD008084. doi: 10.1002/14651858.CD008084.pub4.
16. Eddleston M, Wilks MF, Buckley NA. Prospects for treatment of paraquat-induced lung fibrosis with immunosuppressive drugs and the need for better prediction of outcome: a systematic review. QJM 2003;96:809–824. doi: 10.1093/qjmed/hcg137.
17. Seok SJ, Gil HW, Jeong DS, Yang JO, Lee EY, Hong SY. Paraquat intoxication in subjects who attempt suicide: why they chose paraquat. Korean J Intern Med 2009;24:247–251. doi: 10.3904/kjim.2009.24.3.247.
18. Eddleston M. Patterns and problems of deliberate self-poisoning in the developing world. QJM 2000;93:715–731. doi: 10.1093/qjmed/93.11.715.
19. Zyoud SH. Investigating global trends in paraquat intoxication research from 1962 to 2015 using bibliometric analysis. Am J Ind Med 2018;61:462–470. doi: 10.1002/ajim.22835.
20. Xu NY, Zhang SP, Dong L, Nie JH, Tong J. Proteomic analysis of lung tissue of rats exposed to cigarette smoke and radon. J Toxicol Environ Health A 2009;72:752–758. doi: 10.1080/15287390902841573.
21. Liu D, Mao P, Huang Y, Liu Y, Liu X, Pang X, *et al*. Proteomic analysis of lung tissue in a rat acute lung injury model: identification of prdx1 as a promoter of inflammation. Mediators Inflamm 2014;2014:469358. doi: 10.1155/2014/469358.
22. Ahmad Y, Sharma NK, Ahmad MF, Sharma M, Garg I, Srivastava M, *et al*. The proteome of hypobaric induced hypoxic lung: Insights from temporal proteomic profiling for biomarker discovery. Sci Rep 2015;5:10681. doi: 10.1038/srep10681.
23. Calle EA, Hill RC, Leiby KL, Le AV, Gard AL, Madri JA, *et al*. Targeted proteomics effectively quantifies differences between native lung and detergent-decellularized lung extracellular

matrices. Acta Biomater 2016;46:91–100. doi: 10.1016/j.actbio.2016.09.043.
24. Booth AJ, Hadley R, Cornett AM, Dreffs AA, Matthes SA, Tusi JL, *et al*. Acellular normal and fibrotic human lung matrices as a culture system for in vitro investigation. Am J Respir Crit Care Med 2012;186:866–876. doi: 10.1164/rccm.201204-0754OC.
25. Wang ZY, Ma J, Zhang M, Wen C, Huang X, Sun F, *et al*. Serum metabolomics in rats after acute paraquat poisoning. Biol Pharm Bull 2015;38:1049–1053. doi: 10.1248/bpb.b15-00147.
26. Wang Z, Wang Z, Yu Q, Xi H, Weng J, Du X, *et al*. Comparative study of two perfusion routes with different flow in decellularization to harvest an optimal pulmonary scaffold for recellularization. J Biomed Mater Res A 2016;104:2567–2575. doi: 10.1002/jbm.a.35794.
27. Rangarajan S, Bone NB, Zmijewska AA, Jiang S, Park DW, Bernard K, *et al*. Metformin reverses established lung fibrosis in a bleomycin model. Nat Med 2018;24:1121–1127. doi: 10.1038/s41591-018-0087-6.
28. Hettiarachchi J, Fernando SS. Pulmonary fibrosis following paraquat poisoning. Ceylon Med J 1988;33:141–142.
29. Lacerda AC, Rodrigues-Machado Mda G, Mendes PL, Novaes RD, Carvalho GM, Zin WA, *et al*. Paraquat (pq)-induced pulmonary fibrosis increases exercise metabolic cost, reducing aerobic performance in rats. J Toxicol Sci 2009;34:671–679. doi: 10.2131/jts.34.671.
30. Xie H, Wang R, Tang X, Xiong Y, Xu R, Wu X. Paraquat-induced pulmonary fibrosis starts at an early stage of inflammation in rats. Immunotherapy 2012;4:1809–1815. doi: 10.2217/imt.12.122.
31. Favarel-Garrigues JC. Acute pulmonary fibrosis resulting from ingestion of a herbicide containing paraquat. Bull Physiopathol Respir (Nancy) 1972;8:1289–1294.
32. Smith P, Heath D, Kay JM. The pathogenesis and structure of paraquat-induced pulmonary fibrosis in rats. J Pathol 1974;114:57–67. doi: 10.1002/path.1711140202.
33. Schoenberger CI, Rennard SI, Bitterman PB, Fukuda Y, Ferrans VJ, Crystal RG. Paraquat-induced pulmonary fibrosis. Role of the alveolitis in modulating the development of fibrosis. Am Rev Respir Dis 1984;129:168–173. doi: 10.1164/arrd.1984.129.1.168.
34. Yao R, Cao Y, He YR, Lau WB, Zeng Z, Liang ZA. Adiponectin attenuates lung fibroblasts activation and pulmonary fibrosis induced by paraquat. PLoS One 2015;10:e0125169. doi: 10.1371/journal.pone.0125169.
35. Xu Y, Tai W, Qu X, Wu W, Li Z, Deng S, *et al*. Rapamycin protects against paraquat-induced pulmonary fibrosis: activation of nrf2 signaling pathway. Biochem Biophys Res Commun 2017;490:535–540. doi: 10.1016/j.bbrc.2017.06.074.
36. Rao SS, Zhang XY, Shi MJ, Xiao Y, Zhang YY, Wang YY, *et al*. Suberoylanilide hydroxamic acid attenuates paraquat-induced pulmonary fibrosis by preventing smad7 from deacetylation in rats. J Thorac Dis 2016;8:2485–2494. doi: 10.21037/jtd.2016.08.08.
37. Ohlmeier S, Mazur W, Salmenkivi K, Myllarniemi M, Bergmann U, Kinnula VL. Proteomic studies on receptor for advanced glycation end product variants in idiopathic pulmonary fibrosis and chronic obstructive pulmonary disease. Proteomics Clin Appl 2010;4:97–105. doi: 10.1002/prca.200900128.
38. Korfei M, Schmitt S, Ruppert C, Henneke I, Markart P, Loeh B, *et al*. Comparative proteomic analysis of lung tissue from patients with idiopathic pulmonary fibrosis (ipf) and lung transplant donor lungs.
J Proteome Res 2011;10:2185–2205. doi: 10.1021/pr1009355.
39. Decaris ML, Gatmaitan M, FlorCruz S, Luo F, Li K, Holmes WE, *et al*. Proteomic analysis of altered extracellular matrix turnover in bleomycin-induced pulmonary fibrosis. Mol Cell Proteomics 2014;13:1741–1752. doi: 10.1074/mcp.M113.037267.
40. Carleo A, Bargagli E, Landi C, Bennett D, Bianchi L, Gagliardi A, *et al*. Comparative proteomic analysis of bronchoalveolar lavage of familial and sporadic cases of idiopathic pulmonary fibrosis. J Breath Res 2016;10:026007. doi: 10.1088/1752-7155/10/2/026007.
41. Yang T, Jia Y, Ma Y, Cao L, Chen X, Qiao B. Comparative proteomic analysis of bleomycin-induced pulmonary fibrosis based on isobaric tag for quantitation. Am J Med Sci 2017;353:49–58. doi: 10.1016/j.amjms.2016.11.021.
42. Ahrman E, Hallgren O, Malmström L, Hedström U, Malmström A, Bjermer L, *et al*. Quantitative proteomic characterization of the lung extracellular matrix in chronic obstructive pulmonary disease and idiopathic pulmonary fibrosis. J Proteomics 2018;189:23–33. doi: 10.1016/j.jprot.2018.02.027.
43. Baker EL, Zaman MH. The biomechanical integrin. J Biomech 2010;43:38–44. doi: 10.1016/j.jbiomech.2009.09.007.
44. Huveneers S, Truong H, Fassler R, Sonnenberg A, Danen EH. Binding of soluble fibronectin to integrin alpha5 beta1 - link to focal adhesion redistribution and contractile shape. J Cell Sci 2008;121:2452–2462. doi: 10.1242/jcs.033001.
45. Sheppard D. The role of integrins in pulmonary fibrosis. Eur Respir Rev 2008;17:157–162. doi: 10.1183/09059180.00010909.
46. Furukawa F, Matsuzaki K, Mori S, Tahashi Y, Yoshida K, Sugano Y, *et al*. P38 mapk mediates fibrogenic signal through smad3 phosphorylation in rat myofibroblasts. Hepatology 2003;38:879–889. doi: 10.1053/jhep.2003.50384.
47. Vij R, Noth I. Peripheral blood biomarkers in idiopathic pulmonary fibrosis. Transl Res 2012;159:218–227. doi: 10.1016/j.trsl.2012.01.012.
48. Hoffman SM, Chapman DG, Lahue KG, Cahoon JM, Rattu GK, Daphtary N, *et al*. Protein disulfide isomerase-endoplasmic reticulum resident protein 57 regulates allergen-induced airways inflammation, fibrosis, and hyperresponsiveness. J Allergy Clin Immunol 2016;137:822–832e7. doi: 10.1016/j.jaci.2015.08.018.
49. Kim TH, Lee YH, Kim KH, Lee SH, Cha JY, Shin EK, *et al*. Role of lung apolipoprotein A-I in idiopathic pulmonary fibrosis: antiinflammatory and antifibrotic effect on experimental lung injury and fibrosis. Am J Respir Crit Care Med 2010;182:633–642. doi: 10.1164/rccm.200905-0659OC.
50. Wilberding JA, Ploplis VA, McLennan L, Liang Z, Cornelissen I, Feldman M, *et al*. Development of pulmonary fibrosis in fibrinogen-deficient mice. Ann N Y Acad Sci 2001;936:542–548. doi: 10.1111/j.1749-6632.2001.tb03542.x.
51. Zhang Y, Xin Q, Wu Z, Wang C, Wang Y, Wu Q, *et al*. Application of isobaric tags for relative and absolute quantification (iTRAQ) coupled with two-dimensional liquid chromatography/tandem mass spectrometry in quantitative proteomic analysis for discovery of serum biomarkers for idiopathic pulmonary fibrosis. Med Sci Monit 2018;24:4146–4153. doi: 10.12659/MSM.908702.
52. Landi C, Bargagli E, Carleo A, Refini RM, Bennett D, Bianchi L, *et al*. Bronchoalveolar lavage proteomic analysis in pulmonary fibrosis associated with systemic sclerosis: S100a6 and 14-3-3epsilon as potential biomarkers. Rheumatology (Oxford) 2019;58:165–178. doi: 10.1093/rheumatology/key223.
53. Niu R, Liu Y, Zhang Y, Zhang Y, Wang H, Wang Y, *et al*. Itraq-based proteomics reveals novel biomarkers for idiopathic pulmonary fibrosis. PLoS One 2017;12:e0170741. doi: 10.1371/journal.pone.0170741.
54. Niu R, Li X, Zhang Y, Wang H, Wang Y, Wang W, *et al*. Potential biomarkers of idiopathic pulmonary fibrosis discovered in serum by proteomic array analysis. Int J Clin Exp Pathol 2016;9:8922–8932.

How to cite this article: Wan XL, Zhou ZL, Wang P, Zhou XM, Xie MY, Mei J, Weng J, Xi HT, Chen C, Wang ZY, Wang ZB. Small molecule proteomics quantifies differences between normal and fibrotic pulmonary extracellular matrices. Chin Med J 2020;133:1192–1202. doi: 10.1097/CM9.0000000000000754